

Spectroscopic and transition properties of strontium chloride

Dong-Lan Wu(伍冬兰), Bi-Kun Liu(刘必坤), Wen-Tao Zhou(周文涛), Jia-Yun Chen(陈佳运), Zhang-Li Lai(赖章丽), Bo Liu(刘波), and Bing Yan(闫冰)

Citation: Chin. Phys. B, 2025, 34 (**4**): 043101. DOI: 10.1088/1674-1056/adb264
Journal homepage: http://cpb.iphy.ac.cn; http://iopscience.iop.org/cpb

What follows is a list of articles you may be interested in

Three-body physics under dissipative spin-orbit coupling

Xi Zhao(赵茜)
Chin. Phys. B, 2025, 34 (**3**): 033101. DOI: 10.1088/1674-1056/ada43e

All-electron basis sets for H to Xe specific for ZORA calculations: Applications in atoms and molecules

C. S. Gomes, F. E. Jorge, and A. Canal Neto
Chin. Phys. B, 2024, 33 (**8**): 083101. DOI: 10.1088/1674-1056/ad4bbe

Low-lying electronic states of osmium monoxide OsO

Wen Yan(严汶) and Wenli Zou(邹文利)
Chin. Phys. B, 2023, 32 (**11**): 113101. DOI: 10.1088/1674-1056/acec46

Highly accurate theoretical study on spectroscopic properties of SH including spin-orbit coupling

Shu-Tao Zhao(赵书涛), Xin-Peng Liu(刘鑫鹏), Rui Li(李瑞), Hui-Jie Guo(国慧杰), and Bing Yan(闫冰)
Chin. Phys. B, 2021, 30 (**7**): 073104. DOI: 10.1088/1674-1056/ac003f

Configuration interaction calculations on the spectroscopic and transition properties of magnesium chloride

Dong-lan Wu(伍冬兰), Cheng-quan Lin(林成泉), Yu-feng Wen(温玉锋), An-dong Xie(谢安东), Bing Yan(闫冰)
Chin. Phys. B, 2018, 27 (**8**): 083101. DOI: 10.1088/1674-1056/27/8/083101

DATA PAPER

Spectroscopic and transition properties of strontium chloride

Dong-Lan Wu(伍冬兰)[1,†], Bi-Kun Liu(刘必坤)[1], Wen-Tao Zhou(周文涛)[1], Jia-Yun Chen(陈佳运)[1], Zhang-Li Lai(赖章丽)[1], Bo Liu(刘波)[1,‡], and Bing Yan(闫冰)[2]

[1] *College of Mathematic and Physical, Jinggangshan University, Ji'an* 343009, *China*
[2] *Institute of Atomic and Molecular Physics, Jilin University, Changchun* 130012, *China*

(Received 20 November 2024; revised manuscript received 13 January 2025; accepted manuscript online 5 February 2025)

The spectroscopic and transition properties of strontium chloride (SrCl) are investigated based on the theoretical approach of *ab initio* quantum chemistry. The calculation accuracy is improved by introducing Davidson correction, core-valence correlation (CV), the scalar relativistic and spin–orbit coupling (SOC) effects. The results show that the spectroscopic constants of $X^2\Sigma^+$ and $A^2\Pi$ states are consistent with the experimental results. The spectroscopic and molecular constants of most highly excited electronic states are reported for the first time. The permanent dipole moment (PDMs) and the spin–orbit (SO) matrix element have a sudden change for the avoidance of crossing. The potential energy curves (PECs) of the 14 Λ–S states split into 30 Ω states. The splitting energy of $A^2\Pi$ is 290.76 cm^{-1}, which has a little difference from the experimental value 295.597 cm^{-1}. Finally, the transition properties are given, including transition dipole moment (TDMs), Franck–Canton factor (FCFs) and radiation lifetime. It is found that the calculated radiation lifetime is in the order of 10 ns. The research will provide a theoretical reference for the feasibility of laser cooling of SrCl molecule. The dataset that supported the findings of this study is available in Science Data Bank, with the link https://www.doi.org/10.57760/sciencedb.j00113.00218.

Keywords: SrCl, MRCI + *Q*, spectroscopic and transition properties, spin–orbit coupling

PACS: 31.15.A–, 31.15.vn, 33.15.Mt

DOI: 10.1088/1674-1056/adb264 **CSTR:** 32038.14.CPB.adb264

1. Introduction

Alkaline earth monohalides play an important role in astrophysics, catalysis and high-temperature chemistry.[1–3] In recent years, various spectral results of these molecules have been obtained.[4–7] Among them, strontium atom shows special interest in astrophysics due to its strong absorption lines. Because strontium atom exists in many stars, the spectroscopic study of its halides and monohalides has become a hot topic[8] and the spectroscopic transition properties of strontium halide (Sr*X*) have great reference value in astronomy and astrophysics. Many theoretical and experimental studies have been carried out for alkaline earth monohalides.[9–11] In particular, Brinkmann *et al.*[12] observed the $A^2\Pi$–$X^2\Sigma^+$ transition of SrCl molecule and Schröder *et al.*[13] analyzed the SrCl molecular transition states. Ernst *et al.* studied the high-resolution spectra of $B^2\Sigma^+$–$X^2\Sigma^+$ transition band and gave the main Dunham parameters by fitting.[14] Allouche *et al.*[9] calculated the first four lowest doublet electronic states of SrCl and SrBr molecules using the ligand-field theory, and obtained the energy and spectroscopic constants. The spectroscopic data of the lowest state $X^2\Sigma^+$ of SrCl and SrBr molecules were consistent with those given by Törring *et al.*[15] and listed by Huber and Herzberg.[10] The permanent dipole moments (PDMs) of the first five lowest states were close to those obtained by Törring *et al.*[15] The transition dipole moments (TDMs) were also in agreement with the experimental data.[16,17] Lately, Adem *et al.*[18] gave the spectroscopic constants and the TDMs of the 11 lowest doublet states for SrCl. In all these previous works, the scalar relativistic effect and SOC effect were not fully considered although Davidson correction and core-valence (CV) correlation were involved. This article will use multiple corrections to the potential energy point to obtain more accurate spectroscopic constants, radiative transition probabilities and lifetimes of SrCl. It will provide new reference for further spectroscopic observation and laser cooling of SrCl molecule.

In this paper, we present the calculation of multi-reference configuration interaction method including Davidson correction (MRCI + *Q*). The calculation particularly considers the scalar relativistic effect and SOC effect. The potential energy curves (PECs) of the 14 Λ–S states and 30 Ω states have been calculated and the spectroscopic constants and the transition properties, including TDMs, Franck–Canton factors (FCFs), and the radiative lifetimes, have also been determined. These new accurate data will provide a new reference for further spectroscopic observation and laser cooling of SrCl molecule.

[†]Corresponding author. E-mail: wudonglan1216@sina.com
[‡]Corresponding author. E-mail: liubo@jgsu.eu.cn

© 2025 Chinese Physical Society and IOP Publishing Ltd. All rights, including for text and data mining, AI training, and similar technologies, are reserved.

2. Computational methods

All the *ab initio* calculations are performed on the SrCl system using the computational chemistry program MOLPRO 2012.[19,20] Because of the limit of the MOLPRO program, the C_{2v} point group is used to calculate, which holds $A_1/B_1/B_2/A_2$ irreducible representations. For the SrCl system, $4a_1$, $2b_1$, and $2b_2$ symmetry molecular orbitals are determined as the active space, corresponding to the Sr 4s4p and Cl 3s3p shells. Considering that in the optimization process, the outermost valence electrons and the electrons in the second outer layer are calculated as correlated electrons. In the active space, the outermost electrons of Sr and Cl atoms are placed. The sub-outer electrons of Sr are put in the closed shell. The rest of the inner electrons are put into the core orbitals. That is, there are 17 electrons used in the correlation energy calculations.

In order to obtain the high-level PECs of SrCl, the potential energy point near the equilibrium bond length is calculated with the internally contracted multireference configuration interaction method,[23–26] with the relativistic effective core pseudopotential basis aug-cc-pV5Z-PP (ECP28MWB)[28] for Sr and aug-cc-pV5Z-DK[29] for Cl. The Davidson correction, core-valence correlation, scalar relativistic effect[27] and SOC effect corrections are introduced to improve the calculation accuracy. The SOC effect is corrected with the Breit–Panli Hamiltonian.[30] The off-diagonal SO matrix elements are calculated by using CASSCF wavefunctions, while the diagonal SO matrix elements are substituted with ic-MRCI + Q energies.

Based on the modified PECs, the spectroscopic constants are gained with the aid of the LEVEL8.0 program.[31] The SO matrix elements between electronic states are computed and used to analyze the coupling between the interacting Λ–S states. The TDMs are calculated in the complete active space self-consistent field. The FCFs are evaluated with the LEVEL8.0 program.[31] Finally, the radiative lifetimes are predicted with the obtained TDMs and FCFs.

3. Results and discussion

3.1. The PECs of the Λ–S states

The Λ–S represents the spin and orbital angular momentum quantum number. The theoretical energies of the 14 Λ–S electronic states of SrCl have been calculated as a function of the internuclear distance R from 1.6 Å to 8.0 Å by using the icMRCI + Q method with relativistic effective core pseudopotential aug-cc-pV5Z-PP for Sr and aug-cc-pV5Z-DK for Cl. The potential energy curves (PECs) have been plotted in an interval of points around the equilibrium internuclear distances in Fig. 1. The curves present an irregular form, which suffer from the avoided crossing. Many crossing points between the different states have been obtained and are represented for SrCl in Table 3. As shown in Fig. 1, the 14 Λ–S states are correlated with the three dissociation limits including neutral $Sr(^1S_g) + Cl(^2P_u)$, $Sr(^3P_u) + Cl(^2P_u)$, and ion-pair $Sr^+(^2S_g) + Cl^-(^1S_g)$. And only the $B^2\Sigma^+$ state is associated with the ion-pair limit $Sr^+(^2S_g) + Cl^-(^1S_g)$, which corresponds to the one-electron transfer from Sr to Cl. The three dissociation limits of 14 Λ–S states are listed in Table 1.

By fitting the PECs of $X^2\Sigma^+$, $A^2\Pi$, $B^2\Sigma^+$, $C^2\Pi$ and $3^2\Sigma^+$ bound states, the obtained spectroscopic constants, main electronic configurations and weights around the R_e are listed in Table 2. A comparison with the previous experimental and theoretical results has also been summarized in the table.

As seen, the ground state of SrCl, of $X^2\Sigma^+$ symmetry, has a deep potential well of 3.703 eV, which is separated from the rest of the states and correlated with the lowest dissociation limit $Sr(^1S_g) + Cl(^2P_u)$. The state is mainly characterized by the closed-shell electronic configuration $6\sigma^2 7\sigma^2 8\sigma^\alpha 9\sigma^0 3\pi^2 4\pi^2$, which corresponds to one-electron movement from 3s orbital of Sr to 3p orbital of Cl. For the $X^2\Sigma^+$ state, our calculated R_e and ω_e are in agreement with the recent theoretical calculated results,[18] the deviations are 0.0025 nm and 3.22 cm^{-1}. The calculated B_e is in good agreement with the experimental result,[13] the percentage error is 0%. Compared with other homologues, the calculated D_e (3.703 eV) of SrCl is smaller than 94.31 kcal/mol (4.090 eV) of BeCl[33] and 34283.5 cm^{-1} (4.251 eV)[34] of CaCl. The calculated R_e is 2.575 Å, which is larger than those of BeCl (0.1792 nm),[33] MgCl (0.2214 nm),[35] and CaCl (0.2506 nm).[34] These comparisons indicate that SrCl is more unstable and easier to dissociate than BeCl, MgCl and CaCl.

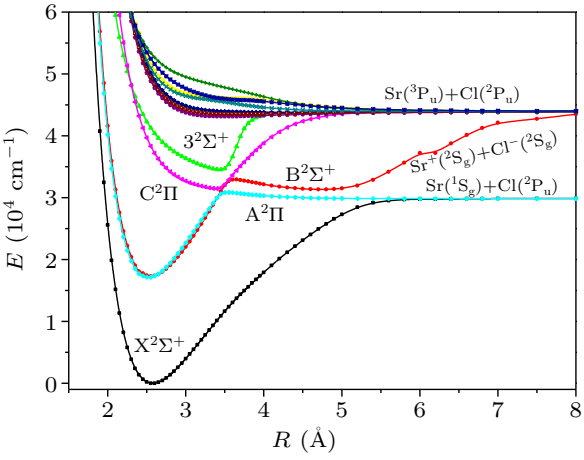


Fig. 1. The PECs of the Λ–S states of SrCl molecule.

Table 1. The dissociation relationships of the Λ–S states of SrCl molecule.[32]

Λ–S	Atomic state
$^2\Sigma^+$, $^2\Pi$	$Sr(^1S_g) + Cl(^2P_u)$
$^{2,4}\Sigma^+(2)$, $^{2,4}\Sigma^-(2)$, $^{2,4}\Pi(2)$, $^{2,4}\Delta$	$Sr(^3P_u) + Cl(^2P_u)$
$^2\Sigma^+$	$Sr^+(^2S_g) + Cl^-(^1S_g)$

Table 2. The spectroscopic constants of of $X^2\Sigma^+$, $A^2\Pi$, $B^2\Sigma^+$, $C^2\Pi$ and $3^2\Sigma^+$ bound states of SrCl molecule.

Λ–S	T_e (cm^{-1})	R_e (nm)	ω_e (cm^{-1})	$\omega_e\chi_e$ (cm^{-1})	B_e (cm^{-1})	$10^{-4}\alpha_e$ (cm^{-1})	D_e (eV)	Main configuration at R_e (%)
$X^2\Sigma^+$	0	0.2575	309.78	0.8682	0.1016	4.131	3.703	$6\sigma^27\sigma^28\sigma^\alpha9\sigma^03\pi^24\pi^2$ (78.8)
								$6\sigma^27\sigma^28\sigma^09\sigma^\alpha3\pi^24\pi^2$ (7.5)
Calc.[18]	0	0.255	313	0.93	0.1037	–	–	
Expt.[14]	0	0.257	302[10]	0.95[10]	–	–	–	
Expt.[13]	0	–	302.448	−0.9502	0.1016	4.524	–	
$A^2\Pi$	15779.16	0.2518	330.69	–	0.1061	2.013	1.673	$6\sigma^27\sigma^28\sigma^09\sigma^03\pi^{\alpha\alpha\beta}4\pi^2$ (85.7)
Calc.[18]	14730	0.252	323	0.95	0.1055	–	–	
Expt.[14]	14818	0.255	309[10]	0.98[10]	–	–	–	
Expt.[13]	14966.73	–	309.625	0.996	0.1030	4.606	–	
$B^2\Sigma^+$	16612.74	0.2538	318.67	0.4874	0.1043	2.599	1.937	$6\sigma^27\sigma^28\sigma^\alpha9\sigma^03\pi^24\pi^2$ (78.8)
								$6\sigma^27\sigma^28\sigma^09\sigma^\alpha3\pi^24\pi^2$ (7.6)
Calc.[18]	15714	0.253	319	0.99	0.1055	–	–	
Expt.[14]	15719	0.255	306[10]	0.98[10]	0.1030[13]	4.739[13]	–	
$C^2\Pi$	33532.99	0.3477	425.57	15.5691	0.0554	−11.932	1.546	$6\sigma^27\sigma^28\sigma^09\sigma^03\pi^{\alpha\alpha\beta}4\pi^2$ (59.7)
								$6\sigma^27\sigma^28\sigma^29\sigma^03\pi^24\pi^2$ (13.4)
								$6\sigma^27\sigma^\alpha8\sigma^\beta9\sigma^03\pi^{\alpha\alpha\beta}4\pi^2$ (9.8)
								$6\sigma^27\sigma^\alpha8\sigma^\alpha9\sigma^03\pi^{\alpha\beta\beta}4\pi^2$ (2.7)
Calc.[18]	26688	0.259	278	0.83	0.1095	–	–	
Expt.[10]	26099	–	270	0.72	–	–	–	
$3^2\Sigma^+$	36625.55	0.3519	392.49	10.4544	0.0544	−12.567	1.140	$6\sigma^27\sigma^\alpha8\sigma^29\sigma^03\pi^24\pi^2$ (51.0)
								$6\sigma^27\sigma^28\sigma^09\sigma^\alpha3\pi^24\pi^2$ (16.4)
								$6\sigma^27\sigma^28\sigma^\alpha9\sigma^03\pi^{\alpha\alpha\beta}4\pi^2$ (4.6)
								$6\sigma^27\sigma^28\sigma^\alpha9\sigma^03\pi^\beta4\pi^{\alpha\alpha\beta}$ (4.6)
								$6\sigma^27\sigma^28\sigma^\alpha9\sigma^03\pi^24\pi^2$ (2.5)
Calc.[18]	27979	0.248	358	1.01	0.1095	–	–	
Expt.[14]	28822	–	3446[10]	1.046[10]	0.1030[13]	–	–	

Apart from the $X^2\Sigma^+$ state, the first excited state $A^2\Pi$ also correlates with $Sr(^1S_g) + Cl(^2P_u)$. The $A^2\Pi$ state is mainly described by the electronic configuration $6\sigma^27\sigma^28\sigma^09\sigma^03\pi^{\alpha\alpha\beta}4\pi^2$, which corresponds to one-electron excitation from the $X^2\Sigma^+$ state, namely, $8\sigma \rightarrow 3\pi$. The calculated T_e of 15779.16 cm^{-1} differs from the experimental value of 14966.73 cm^{-1}, and the percent error is 5.4%.[13] There is an obvious barrier of 30951.13 cm^{-1} owing to an avoided crossing near 0.348 nm. The calculated dissociation energy D_e is 1.673 eV, which is much smaller than that of the ground state. Our computed R_e differs from the experiment[13] by 0.0047 nm. The other spectroscopic constants B_e and ω_e are general consistent with the recent theoretical results,[18] and the deviations 0.0006 cm^{-1} (0.57%) and 7.6 cm^{-1} (2.38%). For the $C^2\Pi$ state, it corresponds to the second neutral dissociation limit $Sr(^3P_u) + Cl(^2P_u)$. The computed D_e of 1.546 eV is slightly smaller than that of the $A^2\Pi$ state. From Fig. 1, we also found that the minimum energy point 31191.10 cm^{-1} is located at the avoided crossing point R_{ACP}, and the energy gap with $A^2\Pi$ state is 239.97 cm^{-1}.

Of particular note is the $B^2\Sigma^+$ state, which is the only state correlating to the ion-pair $Sr^+(^2S_g) + Cl^-(^1S_g)$. The PECs of $B^2\Sigma^+$ state are characterized by a double-well structure, the nuclear distance is 0.2538 nm. The wavefunction of the $B^2\Sigma^+$ state exhibits the obvious multi-configuration character, which consists of two main electronic configurations $6\sigma^27\sigma^28\sigma^\alpha9\sigma^03\pi^24\pi^2$ (78.8) and $6\sigma^27\sigma^28\sigma^09\sigma^\alpha3\pi^24\pi^2$ (7.6) at R_e. The acquired T_e is 16612.74 cm^{-1}, which is also different from the experimental value 15719.5 cm^{-1},[14] and the relative deviation is 5.7%. The spectral constants ω_e, R_e, B_e are also different from the experimental results,[14] but they are also very consistent with the recent theoretical results,[18] and the deviations are only 0.33 cm^{-1}, 0.0008 nm and 0.0012 cm^{-1}, respectively. From Fig. 1, we can also find that there are two intersections at 0.261 nm and 0.340 nm for $A^2\Pi$ and $B^2\Sigma^+$. Few theoretical or experimental studies have reported spectroscopic parameters of other excited electronic states in the literature. The spectroscopic constants calculated in this paper will provide accurate prediction of SrCl molecules.

The permanent electric dipole moments (PDMs) reflect the bonding properties of molecules. The PDMs of the five bound electronic states of SrCl have been plotted as a function of the nuclear spacing R from 1.5 Å to 5.0 Å and depicted in Fig. 2. With the help of the dipole moment curves, we discuss the interactions and polarity of the states. As shown in Fig. 2, many negative values of the moments appearing in the figure are due to the polarity of SrCl. Almost all these moments except for $B^2\Sigma^+$ state lead to the consistent asymptotic limit of 0 a.u. (a.u. represents atomic units), corresponding to the dissociation limit of Sr + Cl. The PDM of $B^2\Sigma^+$ state is negative and shows a linear dependence on R at large bond

distance. When the nuclear spacing increases to 0.57 nm, the maximum dipole moment (4.907 a.u., about 7.5 Debye) is obtained, which indicates that molecular ions have strong properties. It is consistent with the previous analysis of the dissociation limit of the corresponding ion pair $Sr^+ + Cl$. This behavior is obtained also in the study of the low lying electronic states in MgCl molecule[35] (See more details in data on the Science DB).

Another interesting feature to note in Fig. 2 is that there are two pairs of complementary abrupt changes of the PDMs. One is caused by the avoidance of crossing between $A^2\Pi$ state and $C^2\Pi$ state near the nuclear spacing of $R_{1ACP} = 3.46$ Å. The other is caused by the avoidance of crossing between $B^2\Sigma^+$ state and $3^2\Sigma^+$ state around the bond distance of $R_{2ACP} = 3.53$ Å. Such abrupt changes of the PDMs can be explained by that the main electronic configuration of the $A^2\Pi$ state is $6\sigma^2 7\sigma^2 8\sigma^0 9\sigma^0 3\pi^{\alpha\alpha\beta} 4\pi^2$ and the $C^2\Pi$ state becomes $6\sigma^2 7\sigma^2 8\sigma^0 9\sigma^0 3\pi^{\alpha\alpha\beta} 4\pi^2$, the $B^2\Sigma^+$ state is $6\sigma^2 7\sigma^2 8\sigma^0 9\sigma^\alpha 3\pi^2 4\pi^2$ and the $3^2\Sigma^+$ state becomes $6\sigma^2 7\sigma^2 8\sigma^0 9\sigma^\alpha 3\pi^2 4\pi^2$ through R_{ACP}, which can be seen from Fig. 5, thus leading to the abrupt changes in the avoided crossing region.

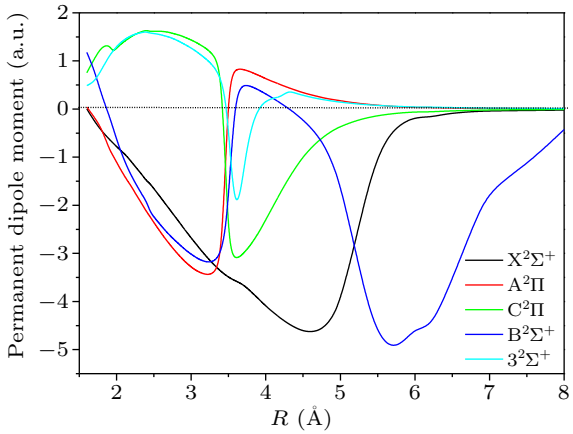


Fig. 2. The PDMs of bound states of SrCl molecule.

3.2. The PECs of the Ω states

The SOC effect could lead to the strong interaction between the adjacent electronic states, especially the states involving the intersection of PECs. And the interaction could be quantitatively evaluated by the spin–orbit (SO) matrix element. The larger spin–orbit matrix element indicates the great interaction between different electronic states. These phenomena in molecules have attracted much research interest in previous investigations.[36–38] Figure 3 only shows the *R*-dependent SO matrix elements of four interaction systems including $B^2\Sigma^+$–$A^2\Pi$, $B^2\Sigma^+$–$C^2\Pi$, $3^2\Sigma^+$–$C^2\Pi$, and $C^2\Pi$–$A^2\Pi$ for SrCl.

The SO matrix elements have the largest values of 300 cm^{-1} for the $3^2\Sigma^+$–$C^2\Pi$ system after the avoided crossing point of the $B^2\Sigma^+$ and $3^2\Sigma^+$ states, indicating the strong interaction between the $3^2\Sigma^+$ and $C^2\Pi$ state. The system $B^2\Sigma^+$–$A^2\Pi$ has larger SO matrix elements 342 cm^{-1}, which is also showing the strong interaction between the $B^2\Sigma^+$ and $A^2\Pi$ states. Therefore, the perturbation of $B^2\Sigma^+$ state is mainly arising from the $A^2\Pi$ and $C^2\Pi$ states, which is consistent with the analysis in the literature.[18] As discussed above, two pairs of the complementary sudden changes have been exhibited, which both result from the PECs' avoided crossings of $B^2\Sigma^+$ and $3^2\Sigma^+$ states, $A^2\Pi$ and $C^2\Pi$ states.

The Ω represents the total angular momentum quantum number. After considering the spin–orbit coupling effect, the 14 Λ–S states split into 30 Ω states, including fifteen $\Omega = 1/2$ states, ten $\Omega = 3/2$ states, four $\Omega = 5/2$ states, and one $\Omega = 7/2$ state. Eight dissociation limits $Sr(^1S_{0g}) + Cl(^2P_{3/2u})$, $Sr(^1S_{0g}) + Cl(^2P_{1/2u})$, $Sr(^3P_{0u}) + Cl(^2P_{3/2u})$, $Sr(^3P_{1u}) + Cl(^2P_{3/2u})$, $Sr(^3P_{2u}) + Cl(^2P_{3/2u})$, $Sr(^3P_{0u}) + Cl(^2P_{1/2u})$, $Sr(^3P_{1u}) + Cl(^2P_{1/2u})$, and $Sr(^3P_{2u}) + Cl(^2P_{1/2u})$ are generated by $Sr(^1S_g) + Cl(^2P_u)$ and $Sr(^3P_u) + Cl(^2P_u)$. The corresponding dissociation relationships are listed in Table 3.

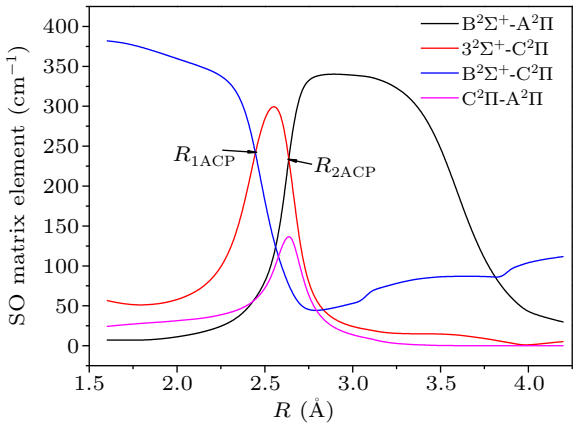


Fig. 3. The *R*-dependent spinorbit matrix elements involving the $A^2\Pi$, $B^2\Sigma^+$, $C^2\Pi$ and $3^2\Sigma^+$ states of SrCl molecule.

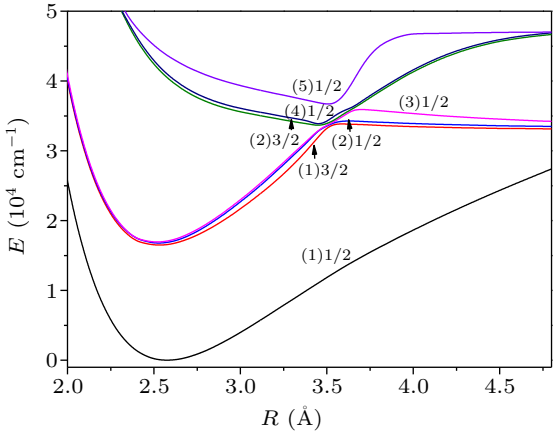


Fig. 4. The PECs of the $\Omega = 1/2$ and $\Omega = 3/2$ bound states of SrCl molecule.

It can be seen from Table 3 that the energy gaps of Sr and Cl in this paper are 14298.110 cm^{-1} for $Sr(^1S_{0g})$–

$Sr(^3P_{0u})$, 201.126 cm^{-1} for $Sr(^3P_{1u})$–$Sr(^3P_u)$, 392.455 cm^{-1} for $Sr(^3P_{2u})$–$Sr(^3P_{1u})$, and 881.680 cm^{-1} for $Cl(^2P_{1/2u})$–$Cl(^2P_{3/2u})$, respectively, which are in good accordance with the corresponding observed values 14317.520 cm^{-1}, 186.831 cm^{-1}, 394.212 cm^{-1} and 882.350 cm^{-1}.[38] Figure 4 shows the PECs of seven bound Ω states, which correspond to four dissociation limits. The spectroscopic constants are fitted with the PECs, and the main Λ–S composition at R_e are listed in Table 4.

When the SOC effect is considered, the compositions of $X^2\Sigma^+_{1/2}$ and $X^2\Sigma^+$ Λ–S states are consistent. The spectroscopic constants are almost unchanged except for the dissociation energy D_e, which is mainly caused by SO splitting of Cl atom. The $A^2\Pi$ state splits into two bound Ω states of 1/2 and 3/2 states. It can be seen that the influence of SOC is mainly reflected in T_e and D_e. The SO splitting energy is 290.76 cm^{-1}, which is in good agreement with the experimental value 295.597 cm^{-1}.[13] The PECs will become complicated after considering the SOC effect and avoiding crossing rule. Due to the abrupt changes of wavefunction at the equilibrium position, the potential energy curve of $\Omega = (3)1/2$ state has partially changed by (2)1/2 and (4)1/2, the $\Omega = (4)1/2$ state by (3)1/2 and (5)1/2. Because of the high state density of the higher-energy states, the SOC leads to stronger mixture of the Λ–S components and more complicated shapes of the PECs, especially for the $\Omega = 1/2$ states. In view of the above, the SOC effects should be taken into account for the spectroscopy study of excited states of SrCl.

Table 3. The dissociation relationships of the Ω states of SrCl molecule.

Ω state	Atomic state	Energy (cm^{-1})	
		this work	Expt.[a]
(1) 1/2, 3/2	$Sr(^1S_{0g})+Cl(^2P_{3/2u})$	0	0
(2) 1/2	$Sr(^1S_{0g})+Cl(^2P_{1/2u})$	881.680	882.350
(3) 1/2, 3/2	$Sr(^3P_{0u})+Cl(^2P_{3/2u})$	14298.110	14317.520
(4) 1/2, 1/2, 3/2, 3/2, 5/2	$Sr(^3P_{1u})+Cl(^2P_{3/2u})$	14499.236	14504.351
(5) 1/2, 1/2, 1/2, 1/2, 3/2, 3/2, 3/2, 5/2, 5/2, 7/2	$Sr(^3P_{2u})+Cl(^2P_{3/2u})$	14891.691	14898.563
(6) 1/2	$Sr(^3P_{0u})+Cl(^2P_{1/2u})$	15179.790	15199.870
(7) 1/2, 1/2, 3/2	$Sr(^3P_{1u})+Cl(^2P_{1/2u})$	15380.916	15386.701
(8) 1/2, 1/2, 3/2, 3/2, 5/2	$Sr(^3P_{2u})+Cl(^2P_{1/2u})$	15773.371	15780.886

[a] Ref. [39].

Table 4. The spectroscopic constants of the bound Ω states of SrCl molecule.

Ω state	T_e (cm^{-1})	R_e (Å)	ω_e (cm^{-1})	$\omega_e\chi_e$ (cm^{-1})	B_e (cm^{-1})	$10^{-4}\alpha_e$ (cm^{-1})	D_e (eV)
$X^2\Sigma^+_{1/2}$	0	2.5765	309.81	0.871	0.1016	4.13	3.658
(2)1/2	16775.74	2.5270	335.18	0.552	0.1053	1.89	2.071
(1)3/2	16484.98	2.5285	313.63	0.121	0.1051	2.13	2.099
(3)1/2	16925.21	2.5180	332.02	−0.112	0.1062	2.59	2.143
(2)3/2	33621.68	3.4510	339.24	9.536	0.0562	−11.84	1.629
(4)1/2	33621.68	3.4510	339.24	9.536	0.0562	−12.03	1.733
(5)1/2	36656.18	3.5200	393.64	10.516	0.0544	−12.50	1.283

3.3. The transition properties and the radiative lifetimes

According to the principle of avoiding crossing, the adjacent Ω states with the same symmetry will have a crossing phenomenon. The absolute values of the transition dipole moments for each transition state are plotted in Fig. 5. For the avoided crossing of $A^2\Pi$ and $C^2\Pi$ states, there are two obvious abrupt changes around R_{1ACP} and R_{2ACP}. One is the (2)1/2–$X^2\Sigma^+_{1/2}$ and (3)1/2–$X^2\Sigma^+_{1/2}$ at $R_{2ACP} = 2.60$ Å, the other is the (1)3/2–$X^2\Sigma^+_{1/2}$ and (2)3/2–$X^2\Sigma^+_{1/2}$ near $R_{1ACP} = 2.50$ Å. At $R < 2.5$ Å, the transition (2)1/2–$X^2\Sigma^+_{1/2}$ and (1)3/2–$X^2\Sigma^+_{1/2}$, arising from $A^2\Pi$–$X^2\Sigma^+$ transition of Λ–S states, both have relatively large TDMs about 1.78 a.u. It is worth noting that the TDMs value of (3)1/2–$X^2\Sigma^+_{1/2}$ transition changes greatly. There is a maximum of 3.55 a.u. at $R = 3.90$ Å, then it tends to zero (See more details in data on the Science DB).

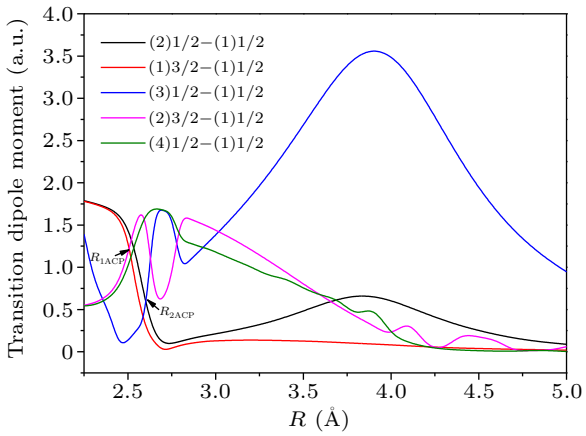


Fig. 5. The TDMs of the lowest five transition states of SrCl molecule.

Table 5. The FCFs of three transition states of SrCl molecule.

	$v''=0$	1	2	3	4	5	6	7	8
					(2)1/2–$X^2\Sigma^+_{1/2}$				
$v'=0$	0.753014	0.211171	0.031543	0.003606	0.000468	0.000120	0.000053	0.000019	0.000002
1	0.209083	0.356953	0.316588	0.093029	0.019037	0.003942	0.001009	0.000285	0.000060
2	0.033753	0.325036	0.101902	0.316260	0.160748	0.047096	0.011602	0.028265	0.000649
3	0.003891	0.090962	0.365704	0.006540	0.241285	0.193469	0.072236	0.019828	0.004839
4	0.000239	0.014518	0.149324	0.321176	0.007600	0.164352	0.206080	0.096694	0.030154
5	0.000017	0.001283	0.008066	0.030817	0.199215	0.241676	0.043850	0.097906	0.204271
6	0.000002	0.000065	0.003883	0.051104	0.236823	0.158727	0.051200	0.045282	0.186741
7	0.000000	0.000011	0.000210	0.008390	0.075696	0.257137	0.087428	0.132627	0.012056
8	0.000000	0.000000	0.000025	0.000620	0.015034	0.103861	0.257938	0.035904	0.16029
					(3)1/2–$X^2\Sigma^+_{1/2}$				
$v'=0$	0.850647	0.270571	0.063763	0.011968	0.002258	0.000553	0.000177	0.000050	0.000006
1	0.275446	0.184407	0.320000	0.154169	0.048440	0.013059	0.003431	0.000855	0.000157
2	0.064468	0.366254	0.010621	0.232605	0.202035	0.087332	0.027546	0.007265	0.001590
3	0.008762	0.147713	0.330492	0.014314	0.131815	0.201237	0.111742	0.040091	0.011060
4	0.000635	0.027878	0.212698	0.231963	0.062896	0.065152	0.188163	0.133996	0.055548
5	0.000037	0.002982	0.053762	0.254468	0.135671	0.110651	0.022792	0.163314	0.151436
6	0.000005	0.000171	0.008030	0.083037	0.271982	0.062738	0.145147	0.002425	0.129021
7	0.000000	0.000022	0.000574	0.015805	0.114900	0.265353	0.018102	0.160569	0.020943
8	0.000000	0.000000	0.000051	0.001538	0.026363	0.147230	0.238532	0.000641	0.156548
					(1)3/2–$X^2\Sigma^+_{1/2}$				
$v'=0$	0.777754	0.186548	0.030128	0.004485	0.000779	0.000205	0.000074	0.000022	0.000002
1	0.199094	0.411687	0.278572	0.083386	0.020384	0.005066	0.001368	0.000360	0.000066
2	0.021955	0.033532	0.157763	0.287292	0.136649	0.044354	0.012544	0.003274	0.000724
3	0.001181	0.061817	0.418108	0.037966	0.237165	0.158080	0.061060	0.018596	0.004850
4	0.000015	0.004517	0.105521	0.420919	0.003247	0.188586	0.167785	0.075699	0.025173
5	0.000001	0.000108	0.009486	0.149232	0.383255	0.002.166	0.146100	0.173012	0.090944
6	0.000000	0.000000	0.000415	0.015706	0.192552	0.330852	0.017886	0.105767	0.171535
7	0.000000	0.000000	0.000000	0.001001	0.024068	0.232337	0.273183	0.043280	0.069526
8	0.000000	0.000000	0.000005	0.000002	0.001857	0.035211	0.265885	0.215115	0.072734

Table 6. The radiative lifetimes of three transition states of SrCl molecule.

Transition	Radiative lifetimes (ns)			
	$v'=0$	$v'=1$	$v'=2$	$v'=3$
(2)1/2–$X^2\Sigma^+_{1/2}$	31.63	31.81	32.04	32.26
Expt.[a)]		31.3 ± 2.7		
(1)3/2–$X^2\Sigma^+_{1/2}$	31.01	31.16	31.52	31.87
Expt.[a)]		30.4 ± 3.6		
(3)1/2–$X^2\Sigma^+_{1/2}$	39.16	39.22	39.31	39.52
Expt.[a)]		38.8 ± 2.1		

[a)] Ref. [16].

The FCFs of the transitions (2)1/2–$X^2\Sigma^+_{1/2}$, (3)1/2–$X^2\Sigma^+_{1/2}$ and (1)3/2–$X^2\Sigma^+_{1/2}$ are calculated and listed in Table 5. By analyzing data, it can be found that three transition states have the largest FCFs for the 0–0 vibrational transition, which are 0.751034, 0.850647 and 0.777754 respectively. And it is also found that the FCFs of (3)1/2–$X^2\Sigma^+_{1/2}$ have significant diagonalization, but the other two are not very obvious. Finally, the radiative lifetimes are calculated by the following formula:[40,41]

$$\tau_{v'} = (A_{v'})^{-1} = \frac{3h}{64\pi^4 |a_0 \cdot e \cdot \overline{\mathrm{TDM}}|_2 \sum_{v''} q_{v',v''} (\Delta E_{v',v''})^3} = \frac{4.936 \times 10^5}{(\overline{\mathrm{TDM}})^2 \sum_{v''} q_{v',v''} (\Delta E_{v',v''})^3},$$

where v' and v'' express the upper and lower vibrational states, $\Delta E_{v',v''}$ is the energy difference, TDM is the averaged electronic transition dipole moment, $q_{v',v''}$ is the FCFs and $\tau_{v'}$ is the radiative lifetime.

The shorter radiative lifetime τ (10^{-9}–10^{-6} s) can provide a significant rate of rapid cycling. The following table lists the radiative lifetimes of $v'=0$–3. The results are all in the order of 10 ns, which are a bit bigger than the experimental results.[16]

4. Conclusion

The PECs and spectroscopic constants of 14 Λ–S states are obtained with ic-MRCI + Q method. The results of $X^2\Sigma^+$ and $A^2\Pi$ states are in good agreement with experimental results. The $B^2\Sigma^+$ state with shallow potential well and large equilibrium internuclear distance, is associated with the ion-pair dissociation limit $Sr^+(^2S_g) + Cl^-(^1S_g)$. The PDMs exhibit two asymptotic limits because of the different dissocia-

tion products of $Sr + Cl$ and $Sr^+ + Cl^-$ at large distance. At the avoided intersection, sudden changes of PDMs and SO reveal the sharp changes of the electron configurations in $A^2\Pi$ and $C^2\Pi$ states. The SOC effect causes 14 Λ–S states to split into 30 Ω states, and many avoided crossings of the PECs are generated. The splitting energy of $A^2\Pi$ state is 290.76 cm^{-1}, which is consistent with the experimental value 295.597 cm^{-1}. At last, the TDMs, FCFs, and radiative lifetimes are calculated. The radiation lifetimes of the three transition bands are all at the level of 10 ns, which conforms to the laser cooling principle. The calculation work in this paper gives the spectroscopic parameters of SrCl molecule, which will provide a reference for further experimental research on molecular laser cooling.

Data availability statement

The data that support the findings of this study are openly available in Science Data Bank at the following link https://www.doi.org/10.57760/sciencedb.j00113.00218.

Acknowledgments

Project supported by the National Natural Science Foundation of China (Grant Nos. 11564019, 11147158, and 12464032) and the Department of Education Foundation of Jiangxi Province of China (Grant No. GJJ2401520).

References

[1] Micheli A, Brennen G and Zoller P 2006 *Nat. Phys.* **2** 341
[2] Baron J, Campbell W, DeMille D, Doyle J M, Gabrielse G, Gurevich Y V, Hess P W, Hutzler N R, Kirilov E, Kozyryev I, O'Leary B R, Panda C D, Parsons M F, Petrik E S, Spaun B, Vutha A C and West A D 2014 *Science* **343** 269
[3] Krems R V 2008 *Phys. Chem. Chem. Phys.* **10** 4079
[4] Törring T, Doebl K and Weiler G 1985 *Chem. Phys. Lett.* **117** 539
[5] Hansen C J, Bergemann M, Cescutti G, Francois P, Arcones A, Karakas A I, Lind K and Chiappini C 2013 *Astronom. Astrophys.* **551** A57
[6] Bergemann M, Hansen C J, Bautista M and Ruchti G 2012 *Astronom. Astrophys.* 546 A90
[7] Caffau E, Andrievsky S, Korotin S, Origlia L, Oliva E, Sanna N, Ludwig H G and Bonifacio P 2016 *Astronom. Astrophys.* **585** A16
[8] Li R, Zhang X M, Feng W, Jiang Y F, Fei D H, Jin M X, Yan B and Xu H F 2014 *Comput. Theor. Chem.* **1032** 20
[9] Allouche A R, Wannous G and Aubert-Frécon M A 1993 *Chem. Phys.* **170** 11
[10] Huber K P and Herzberg G 1979 *Molecular spectra & molecular structure, Constants of Diatonic Molecules*, Vol. IV, Van Nostrand Reinhold, New York
[11] Pandey R K, Waters K, Nigam S, He H, Pingale S S, Pandey A C and Pandey R 2014 *Comput. Theor. Chem.* **1043** 24
[12] Brinkmann U, Schmidt V H and Telle H 1982 *Chem. Phys.* **64** 19
[13] Schröder J O, Zeller B and Ernst W E 1988 *J. Mol. Spectrosc.* **127** 255
[14] Ernst W E and Schröder J O 1984 *J. Chem. Phys.* **81** 136
[15] Törring T, Ernst W E and Kändler J 1989 *J. Chem. Phys.* **90** 4927
[16] Dagdigian P J, Cruse H W and Zare R N 1974 *J. Chem. Phys.* **60** 2330
[17] Berg L E, Royen P and Weijnitz P 1990 *Mol. Phys.* **69** 385
[18] Adem Z, Makhlouf S and Taher F 2016 *Comput. Theor. Chem.* **1093** 48
[19] Werner H J, Knowles P J, Lindh R, *et al.* 2012 MOLPRO, version 2012.1, a package of *ab initio* programs
[20] Werner H J, Knowles P J, Knizia G, Manby F R and Schütz M 2012 *WIREs Comput. Mol. Sci.* **2** 242
[21] Werner H J and Knowles P J 1985 *J. Chem. Phys.* **82** 5053
[22] Knowles P J and Werner H J 1985 *Chem. Phys. Lett.* **115** 259
[23] Werner H J and Knowles P J 1988 *J. Chem. Phys.* **89** 5803
[24] Knowles P J and Werner H J 1988 *Chem. Phys. Lett.* **145** 514
[25] Li R, Wei C L, Sun Q X, Sun E P, Xu H F and Yan B 2013 *J. Phys. Chem. A* **117** 2373
[26] Li R, Zhang X M, Jin M X, Yan B and Xu H F 2014 *Chem. Phys. Lett.* **594** 6
[27] Langhoff S R and Davidson E R 1974 *Int. J. Quantum Chem.* **8** 61
[28] Peterson K A, Figgen D, Goll E, Stoll H and Dolg M 2003 *J. Chem. Phys.* **119** 11099
[29] Wilson A K, Woon D E, Peterson K A and Dunning T H 1999 *J. Chem. Phys.* **110** 7667
[30] Berning A, Schweizer M, Werner H J, Knowles P J and Palmieri P 2000 *Mol. Phys.* **98** 1823
[31] Le Roy R J 2007 LEVEL 8.0: A Computer Program for Solving the Radial Schrdinger Equation for Bound and Quasibound Levels, University of Waterloo Chemical Physics Research Report CP-663, University of Waterloo, Ontario
[32] Zhu Z H 1996 *Atomic and Molecular Reaction Static Mechanics*, Science Press, China
[33] Lima J C B D and Ornellas F R 2013 *J. Mol. Spectrosc.* **283** 22
[34] Fu M K, Ma H T, Cao J W and Bian W S 2016 *J. Chem. Phys.* **144** 184302
[35] Wu D L, Lin C Q, Wen Y F, Xie A D and Yan B 2018 *Chin. Phys. B* **27** 083101
[36] Zhao S T, Yan B, Li R, Wu S and Wang Q L 2017 *Chin. Phys. B* **26** 023105
[37] Wan M J, Jin C G, Yu Y, Huang D H and Shao J X 2017 *Chin. Phys. B* **26** 033101
[38] Wei C L, Zhang X M, Ding D J and Yan B 2016 *Chin. Phys. B* **25** 013102
[39] Moore C E 1971 *Atomic Energy Levels*, National Bureau of Standards, Washington, DC
[40] Okabe H 1978 *Photochemistry of Small Molecules*, Wiley-Interscience, New York
[41] Zou W L and Liu W J 2005 *J. Comput. Chem.* **26** 106